Supporting information

One-step, rapid fluorescent sensing of fungal viability based on a bioprobe with aggregation-induced emission characteristics

Xiaoxue Ge,[†ab] Meng Gao,[†c] Bo Situ,[†ab] Weiwei Feng,[ab] Bairong He,[ab] Xiaojing He,[ab] Shiwu Li,[d] Zihao Ou,[ab] Yiqi Zhong,[ab] Yahui Lin,[ab] Xinyi Ye,[ab] Xiumei Hu,[ab] Ben Zhong Tang[def] and Lei Zheng*[ab]*

[a.]Department of Laboratory Medicine, Nanfang Hospital, Southern Medical University, Guangzhou, 510515, China
[b.]Guangdong Engineering and Technology Research Center for Rapid Diagnostic Biosensors, Nanfang Hospital, Southern Medical University, Guangzhou, 510515, China
[c.]National Engineering Research Center for Tissue Restoration and Reconstruction, South China University of Technology, Guangzhou, 510006, China
[d.]Center for Aggregation-Induced Emission, State Key Laboratory of Luminescent Materials and Devices, South China University of Technology, Guangzhou, 510640, China
[e.]Department of Chemistry, Hong Kong Branch of Chinese National Engineering Research Center for Tissue Restoration and Reconstruction, The Hong Kong University of Science & Technology, Clear Water Bay, Kowloon, Hong Kong, China
[f.]HKUST Shenzhen Research Institute, No. 9 Yuexing 1st RD, South Area, Hi-tech Park, Nanshan, Shenzhen, 518057, China
† These authors contributed equally to this work.
Corresponding authors: nfyyzhenglei@smu.edu.cn (L.Z.), tangbenz@ust.hk (B.Z.T.)

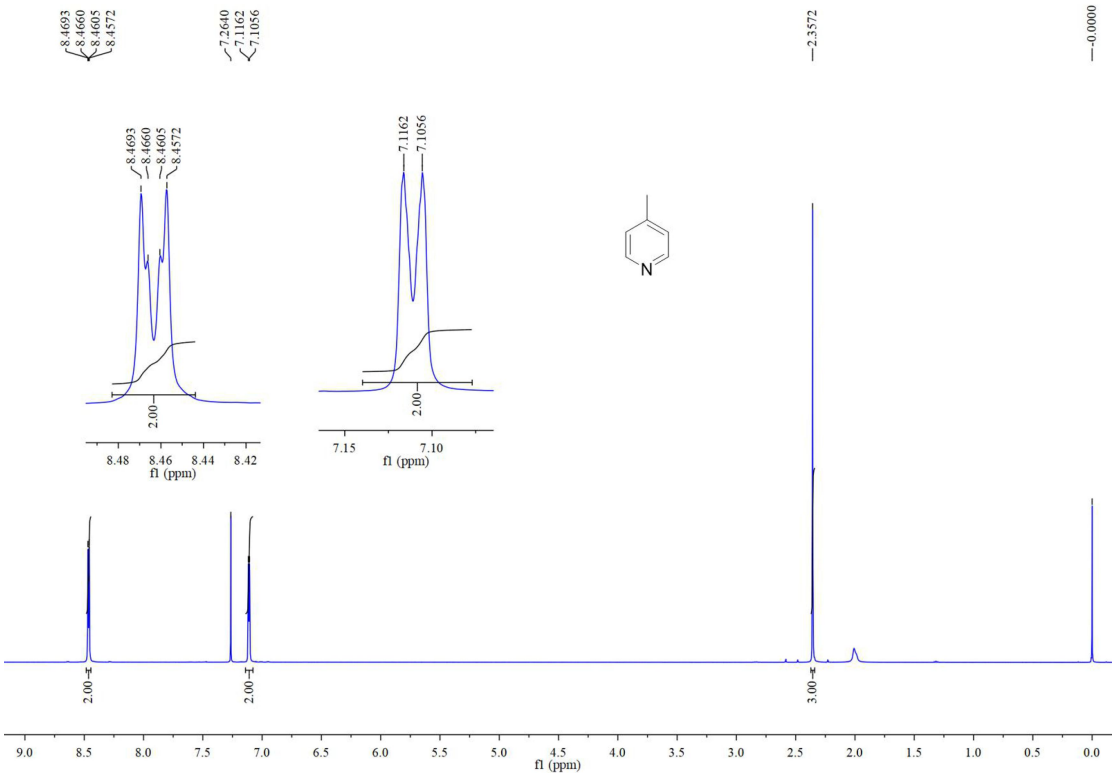

Fig. S1 ^{1}H NMR of compound **1** (500 MHz, $CDCl_3$).

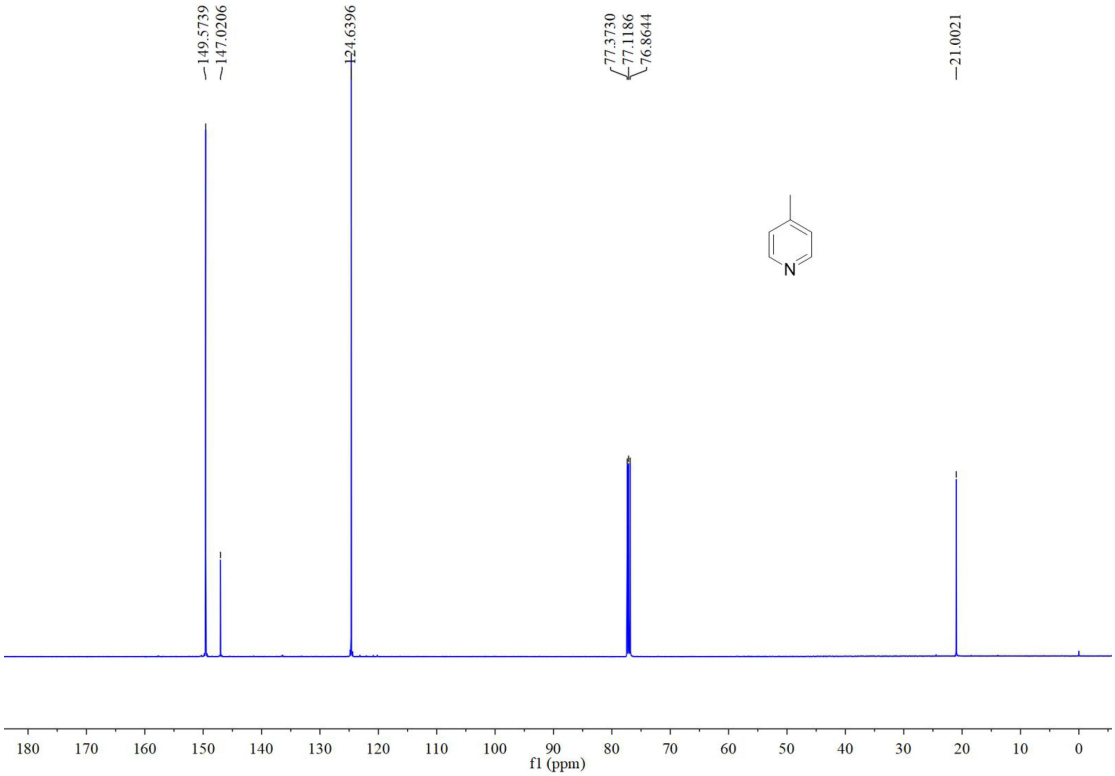

Fig. S2 ^{13}C NMR of compound **1** (125 MHz, $CDCl_3$).

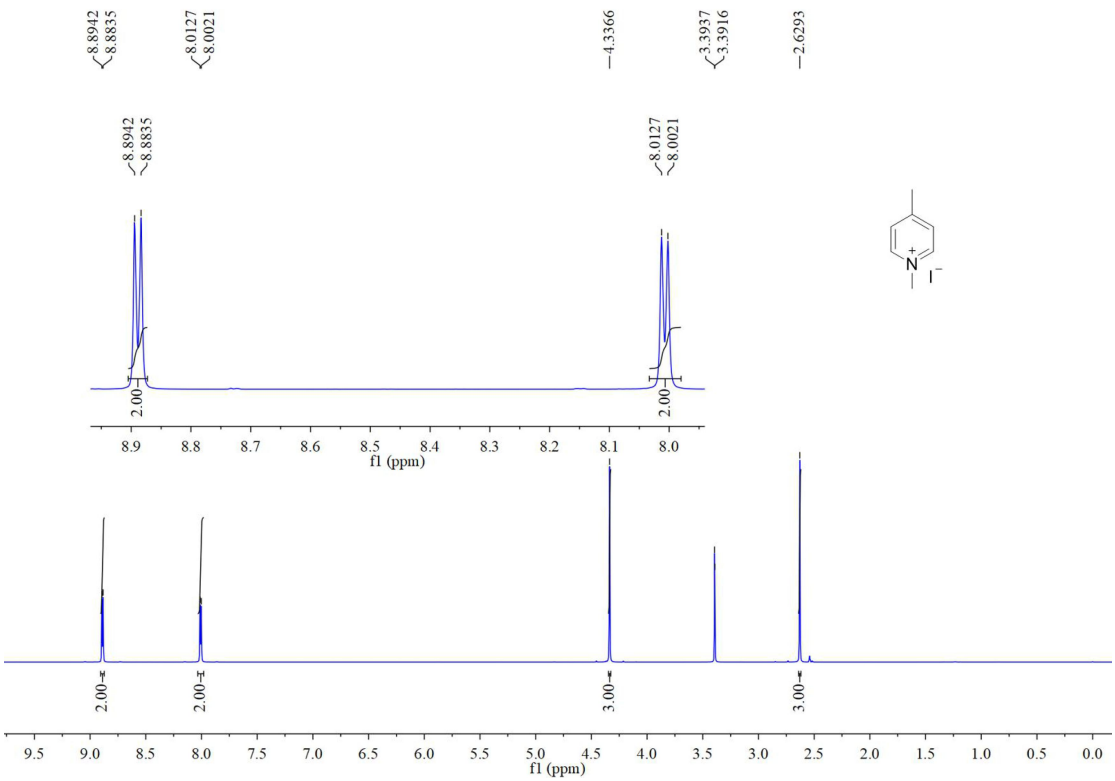

Fig. S3 ^{1}H NMR of compound **2** (600 MHz, DMSO-d_6).

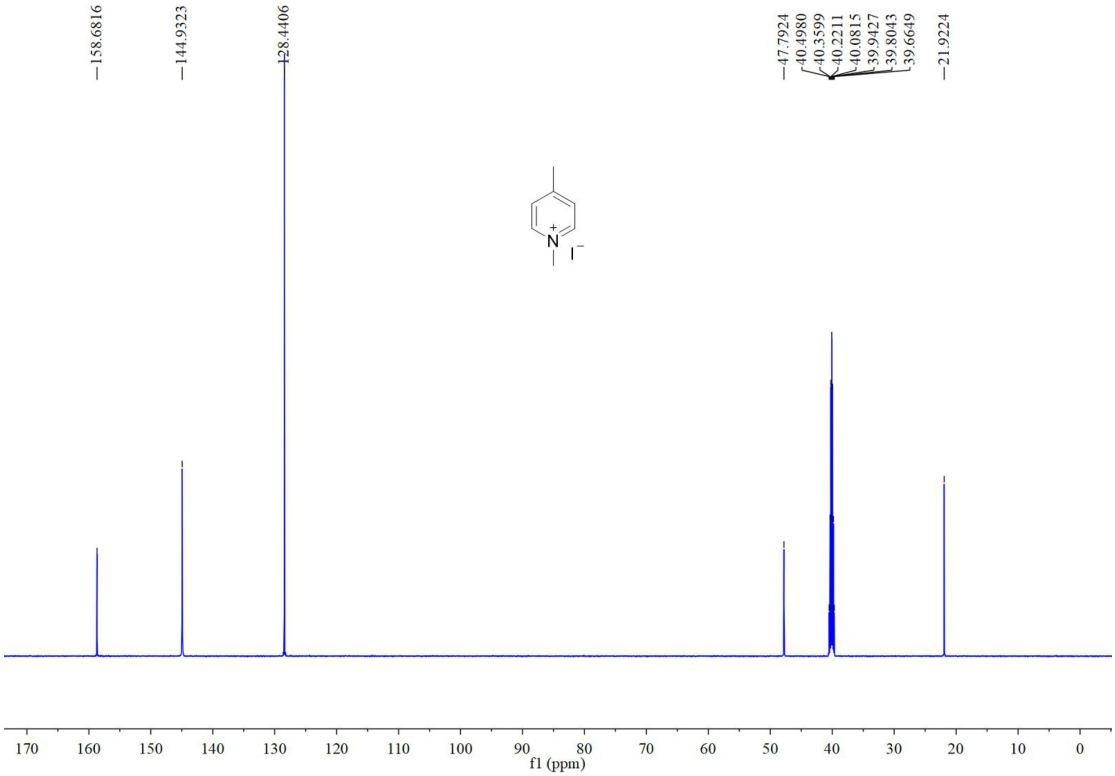

Fig. S4 ^{13}C NMR of compound **2** (150 MHz, DMSO-d_6).

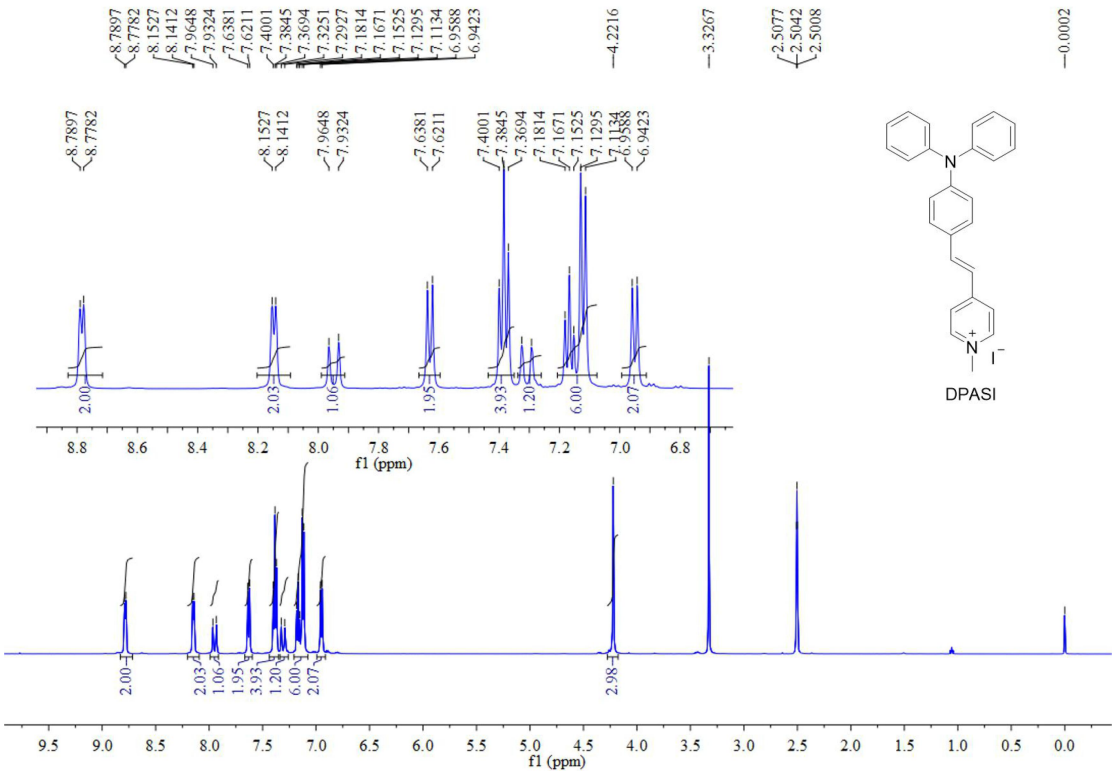

Fig. S5 ^{1}H NMR of DPASI (500 MHz, DMSO-d_6).

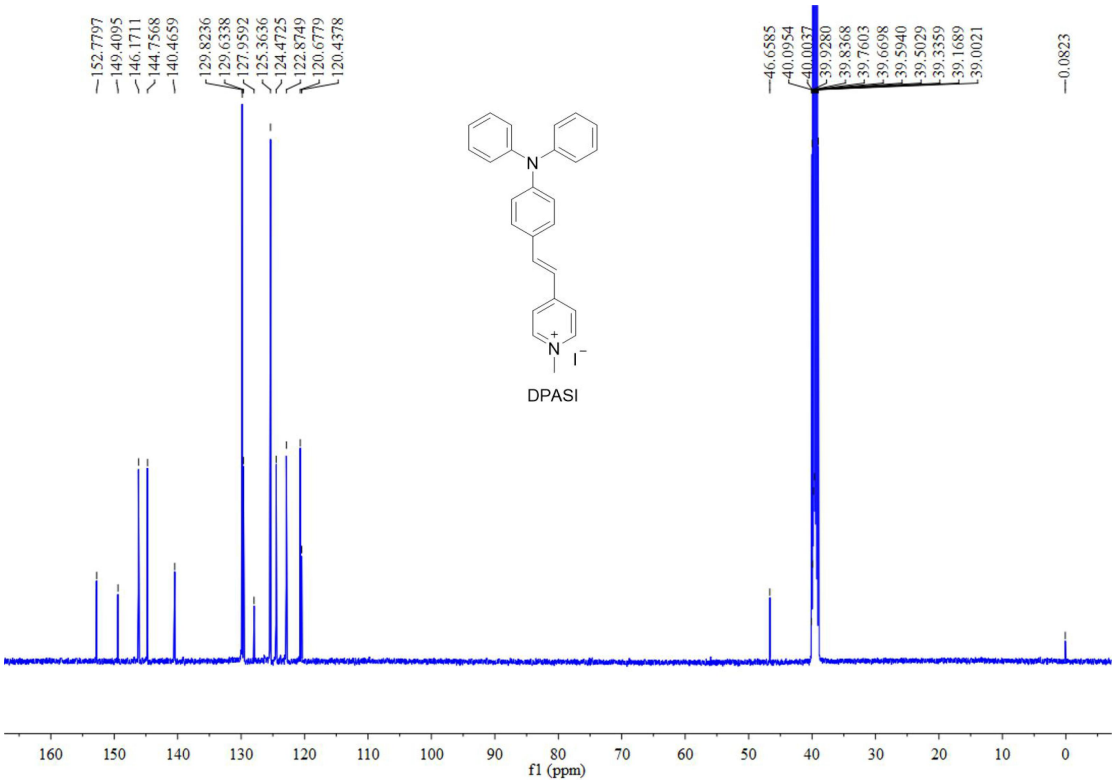

Fig. S6 ^{13}C NMR of DPASI (125 MHz, DMSO-d_6).

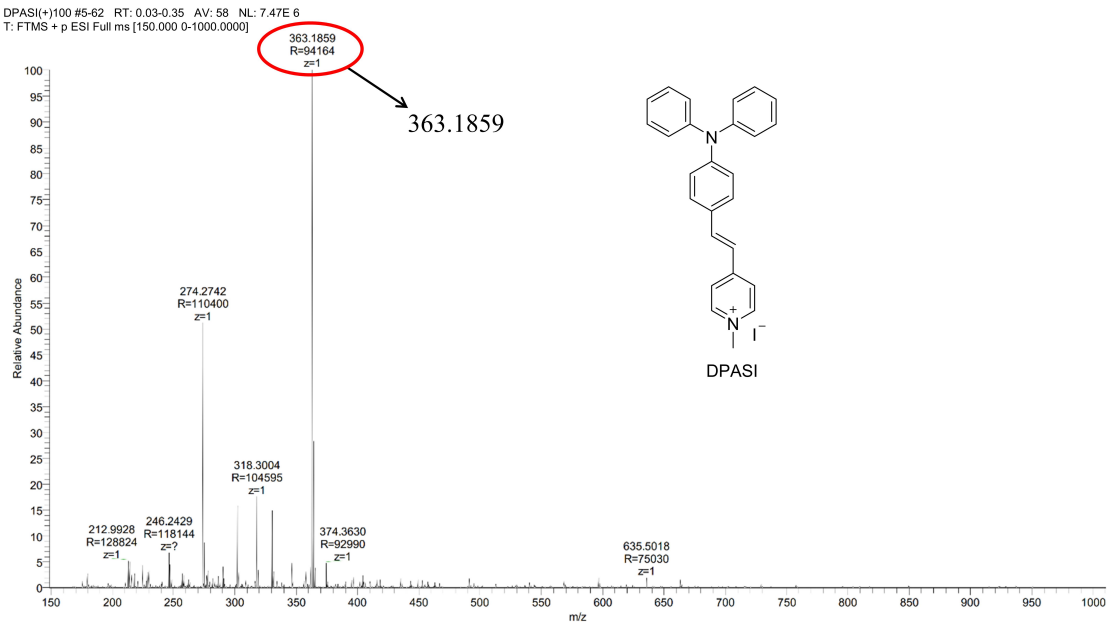

Fig. S7 High resolution mass spectra of DPASI.

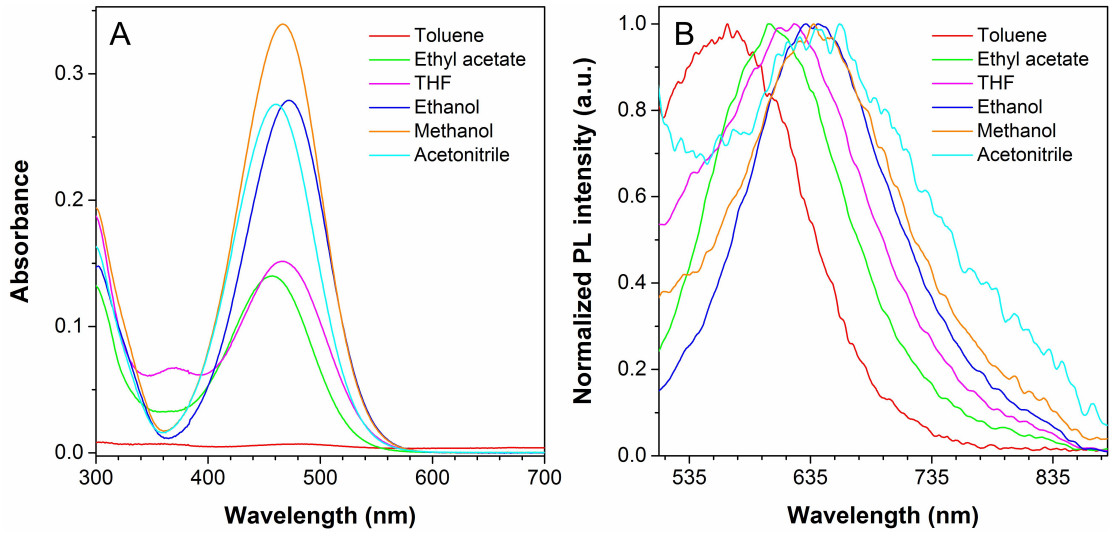

Fig. S8 (A) UV-vis absorption spectra of DPASI (10 μM) in solvents with different polarities. (B) PL spectra of DPASI (10 μM) in solvents with different polarities. λ_{ex} = 467 nm.

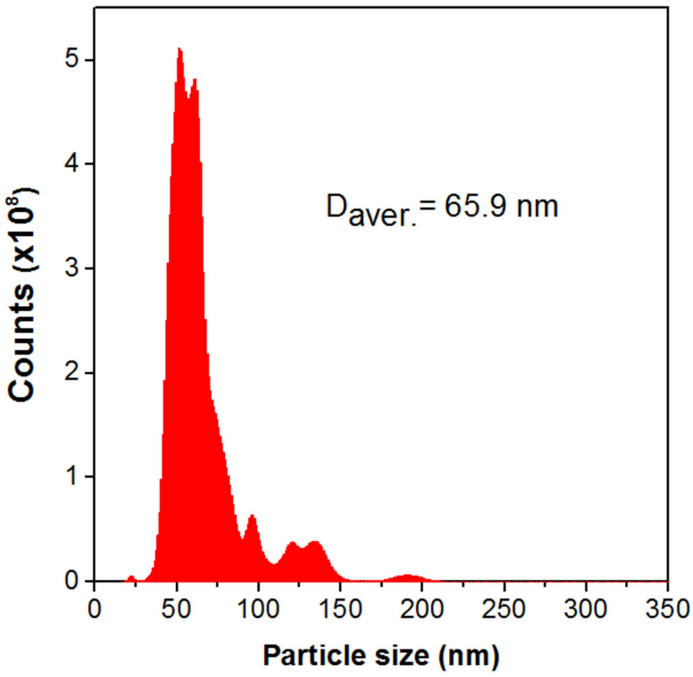

Fig. S9 Particle size of aggregates of DPASI (10 μM) formed in phosphate buffer.

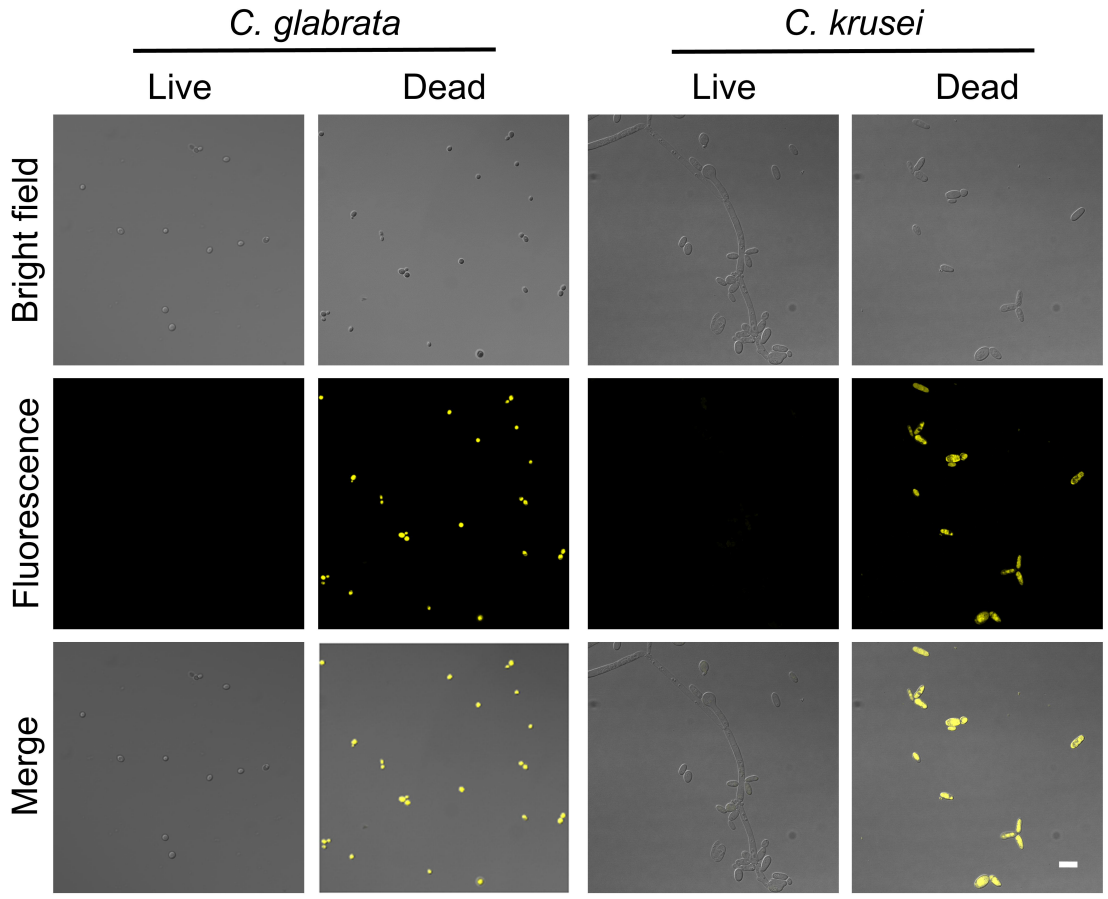

Fig. S10 CLSM images of *C. glabrata* and *C. krusei* stained with 10 μM DPASI. λ_{ex} = 488 nm; Scale bar = 10 μm.

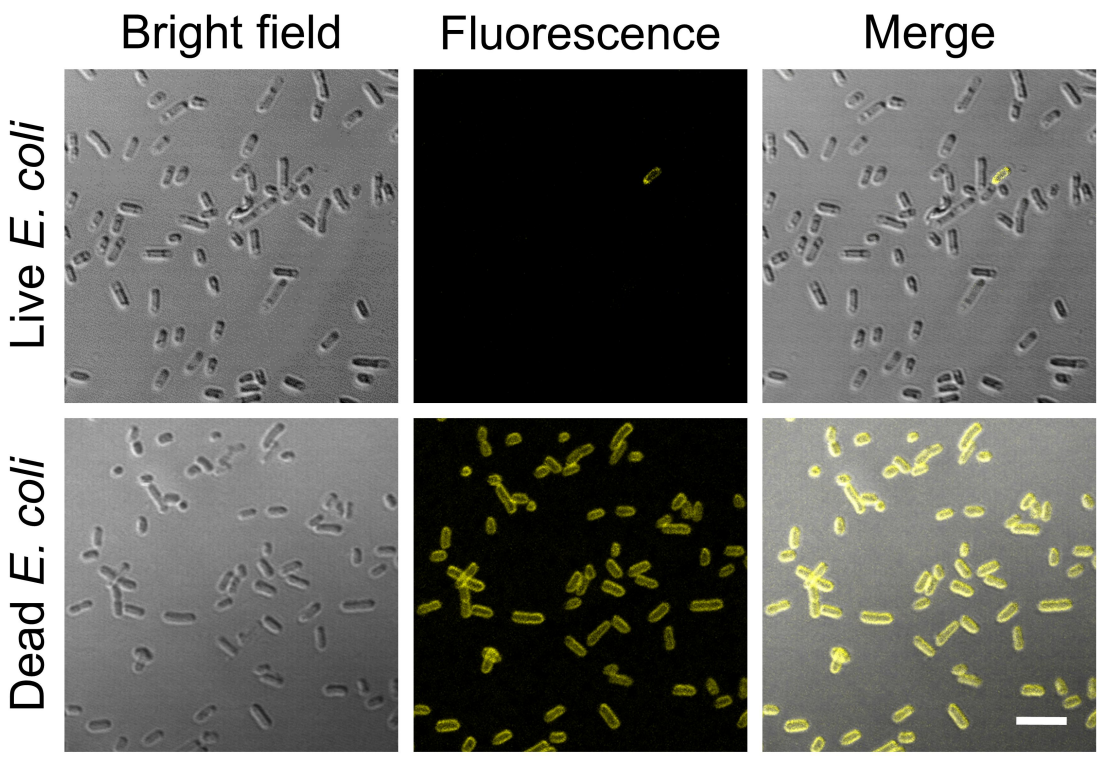

Fig. S11 CLSM images of live and dead (treated with 75% ethanol for 15 minutes) *E. coli* stained with10 μM DPASI. λ_{ex} = 488 nm; Scale bar = 5 μm.

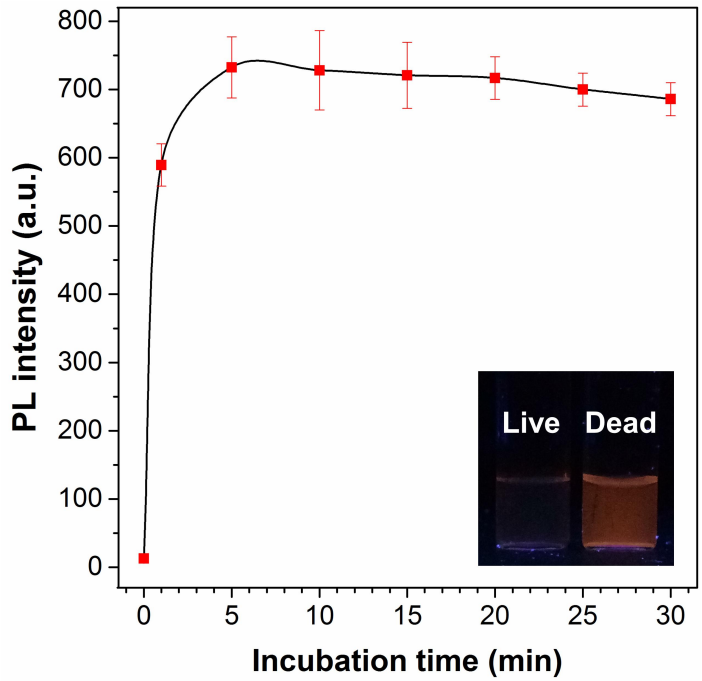

Fig. S12 Change in the PL intensity of DPASI in *C. albicans* suspensions *versus* different incubation time. [DPASI] = 10 μM; λ_{ex} = 467 nm. Inset: Fluorescence photograph of DPASI in *C. albicans* suspensions taken under 365 nm UV irradiation. Error bars indicate the standard error of mean (± SEM).

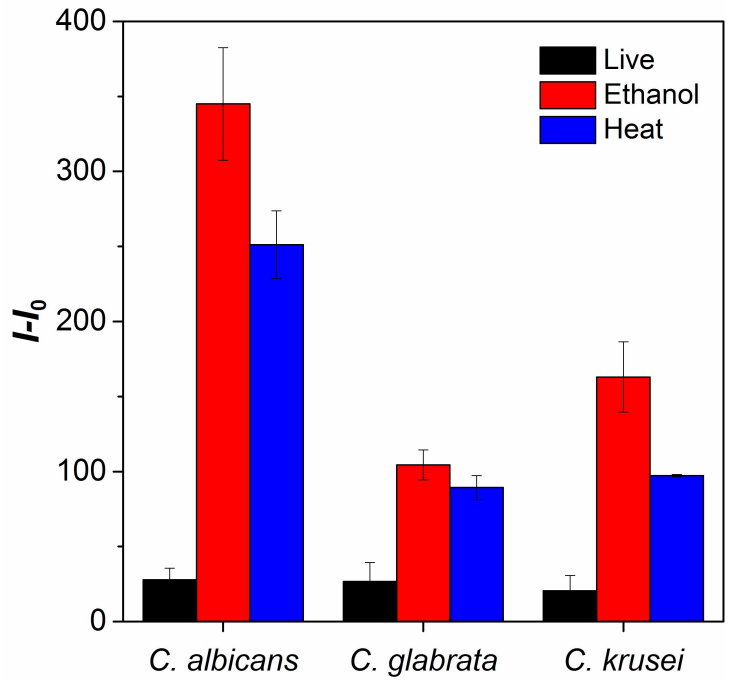

Fig. S13 Fluorescence intensity of *Candidas* suspensions with different treatment followed by staining with DPASI (10 μM); λ_{ex} = 467 nm. Error bars indicate the standard error of mean (± SEM).

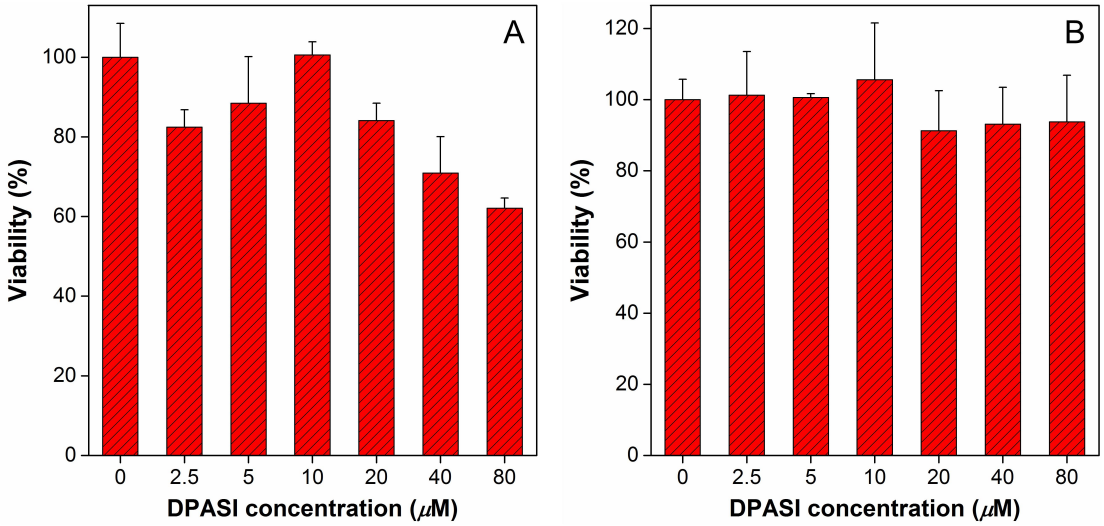

Fig. S14 Viability of *C. glabrata* (A) and *C. krusei* (B) in the presence of different concentrations of DPASI determined by counting after 2-hours or 1-hour incubation, respectively. Error bars indicate the standard error of mean (± SEM).

Additional supporting movie

Movie S1. Representative 3D image of the boxed *Candida* cell in Fig. 5 stained by DAPI, Calcofluor White Staining, and DPASI under SIM excited by 405 nm and 488 nm laser.